Supporting Information

High-Quality Large-Area Graphene from Dehydrogenated Polycyclic Aromatic Hydrocarbons

Xi Wan[1#], Kun Chen[1#], Danqing Liu[2], Jian Chen[3], Qian Miao[2], Jianbin Xu[1*]

[1] Department of Electronic Engineering and Materials Science and Technology Research Center, The Chinese University of Hong Kong, Hong Kong SAR, P. R. China

[2] Department of Chemistry, The Chinese University of Hong Kong, Hong Kong SAR, P. R. China

[3] Instrumental Analysis and Research Center, Sun Yat–sen University, Guangzhou, 510275, P. R. China.

We refer to the graphene sheets grown from coronene, pentacene, and rubrene at 1000˚C as "GC1000", "GP1000" and "GR1000", respectively.

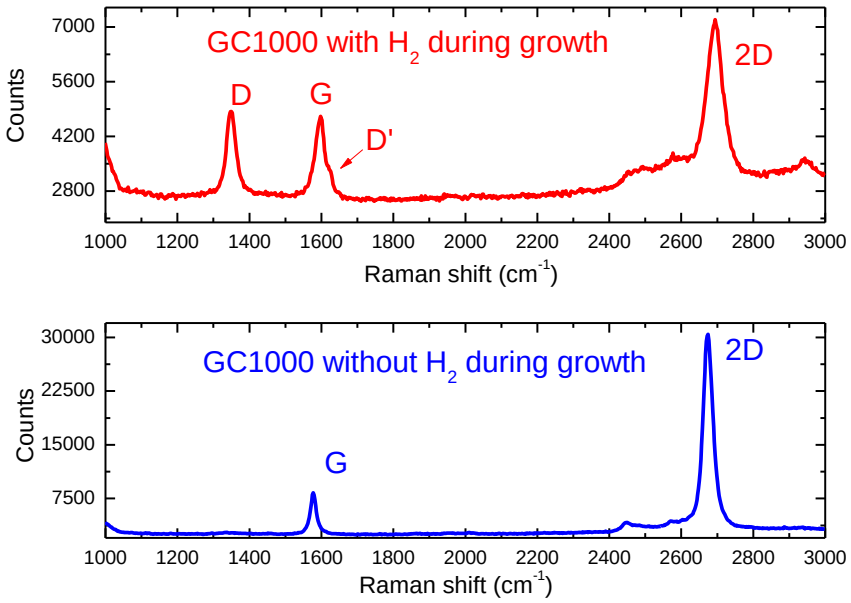

FIGURE S1. Raman spectra of GC1000 with/without H_2 during the graphene growth process

* To whom correspondences should be addressed, jbxu@ee.cuhk.edu.hk

# These authors contributed equally to this work.

SI-1 Transfer of graphene sheets.

A typical transfer process is as follows: (1) spin coating a poly-methyl methacrylate (PMMA) (3000 rpm for 1 min, 5%-9% wt., in anisole); (2) bake the sample at 170 ˚C for 3-5min; (3) etch the Cu foil in Marble's reagent ($CuSO_4$ ~20g, HCl ~100 mL, H_2O ~100 mL) for 3-5hrs; (4) dredge up the floating film with a clean glass substrate and transfer the film into DI water to remove the etchant ions; (5) transfer the film onto a desired substrate and dry it on a hot plate; (6) dip the film into acetone to remove the PMMA layer and dry it with N_2 gas.

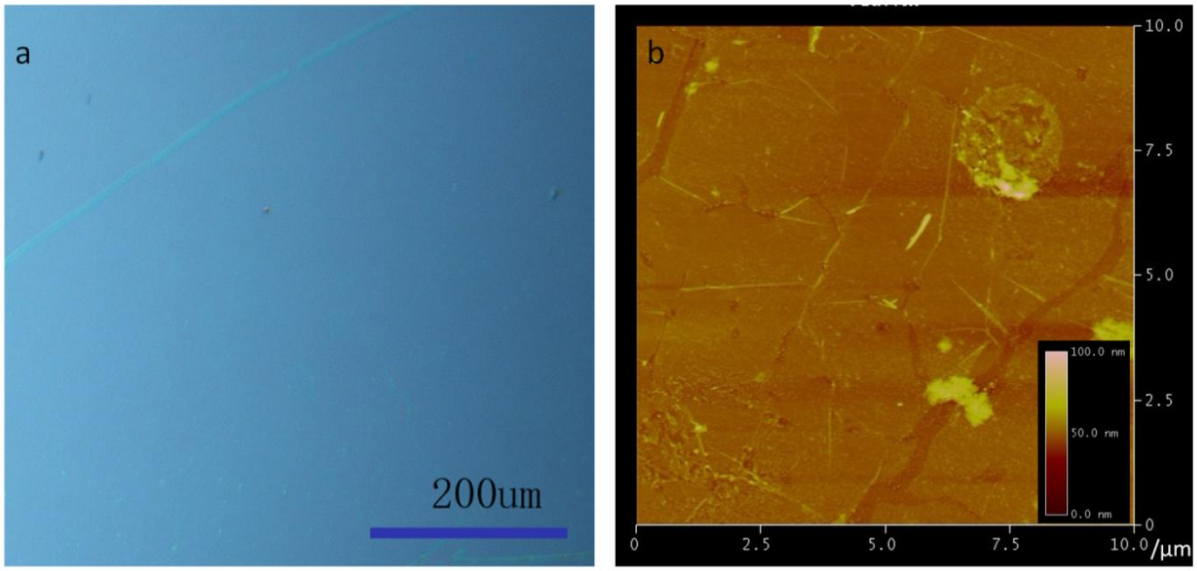

FIGURE S2. (a) An optical micrograph of graphene sheet transferred onto SiO_2/Si substrate with a wrinkle; (b) An AFM image of transferred graphene sheet onto SiO_2/Si substrate, showing some wrinkles/cracks and organic residues.[1]

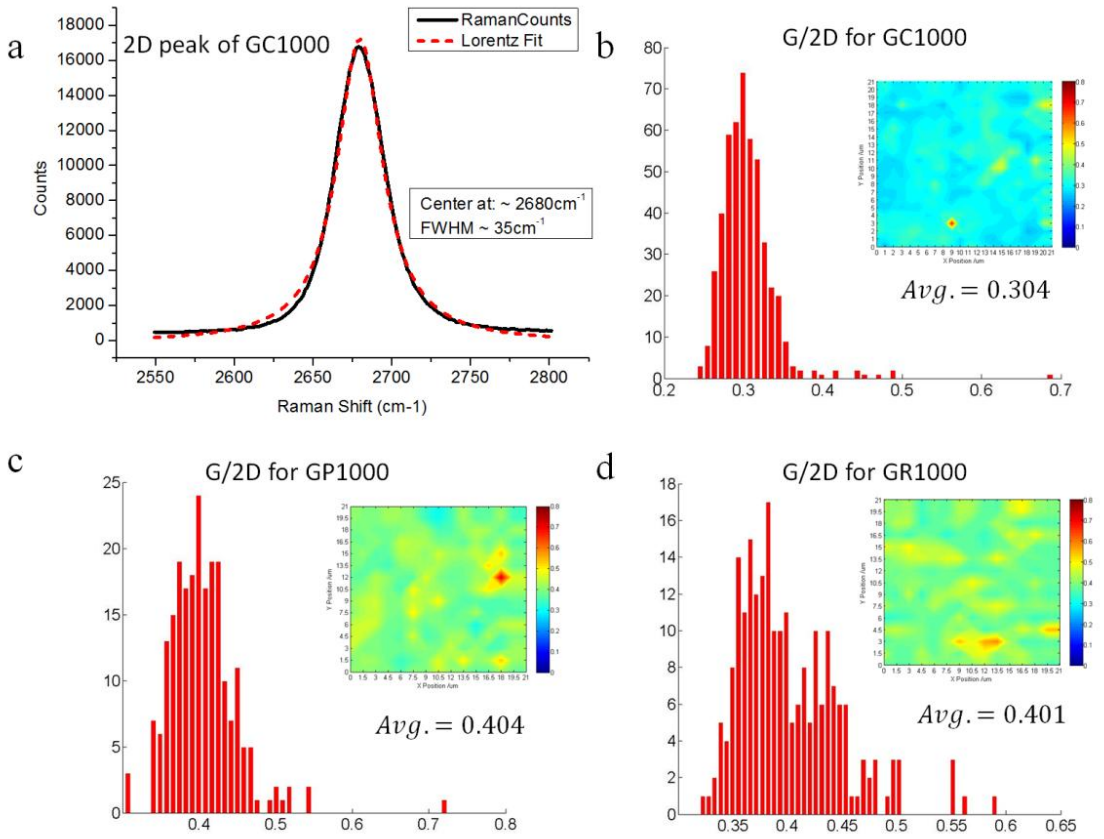

FIGURE S3. (a) Raman 2*D* peak fitting of monolayer graphene (GC1000) with a single Lorentzian peak centered at ~2680 $cm^{-1}$with a full width at half maximum of ~35cm^{-1}. Insets in (b)-(d), *G*/2*D* mapping data of GC1000, GP1000 and GR1000, respectively, colorbar 0 (blue) – 0.8 (red); (b)-(d), histograms of *G*/2*D* mapping data of GC1000, GP1000 and GR1000, respectively. The coverage ratios of monolayer graphene are estimated to be 99.8%, 96.4% and 96.9% for GC1000, GP1000 and GR1000, respectively. The average *G*/2*D* intensity ratios among GC1000, GP1000 and GR1000 are 0.304, 0.404 and 0.401, respectively.

GFET(No.)	L/W	V_{ds}	μ(hole) $cm^2 V^{-1}s^{-1}$	μ(electron) $cm^2 V^{-1}s^{-1}$
No.1	0.1418	50mV	4015	4009
No.2	0.5333	50mV	3464	3312
No.3	0.7124	50mV	2531	1659
No.4	0.3594	50mV	**5366**	**5334**
No.5	0.9478	50mV	3343	2685
No.6	0.1588	50mV	3704	3629

Table T1. The carrier mobility values of our 6 graphene (GC1000) FETs with 300-nm thick SiO_2 dielectric, ranging from 2500 ~ 5300 $cm^2 V^{-1}s^{-1}$ for holes and 1600 ~ 5300 $cm^2 V^{-1}s^{-1}$ for electrons.

SI-2: Details for *ab* initio calculations.

All of the ab initio molecular dynamics (MD) simulations were carried out under the microcanonical ensemble using the Nosé thermostat for temperature control with a time step of 1 fs adopted as the numerical integration algorithm for the equation of motion (EOM). The forces acting on the atoms were calculated from the ground-state electronic energies according to the Hellmann–Feynman theorem at each time step and subsequently used in the integration of Newton's equation of motion. All calculations were performed with the valence orbitals expanded in a plane-wave basis up to a kinetic energy of 400eV. All structures were surrounded by 6 Å of vacuum space in all directions ($\pm x$, $\pm y$, $\pm z$) to ensure that they did not interact with their periodic neighbors. The molecule configuration relaxation was performed in the framework of DFT within the generalized gradient approximation, with the exchange-correlation functional of Perdew and Wang. The linear tetrahedron method (LTM) with Blöchl corrections was used for the Brillouin zone integrations, with 4×4×4 Monkhorst–Pack *k*-point mesh.

For *ab initio* atomistic simulations of PAHs reaction on Cu (111), the first-

principles calculations, based on DFT,[2,3] were performed using the Perdew− Burke− Ernzerhof (PBE) functional within the generalized gradient approximation (GGA) was used to describe the exchange− correlation interactions.[4] And Projector-augmented wave (PAW) pseudopotentials were used to describe the core electrons.[5] All calculations were done using VASP code.[6] The wave functions were expanded in plane waves up to a cutoff of 400 eV. The Cu(111) surface was modeled in a repeated slab geometry: a slab of two Cu(111) layers and 15 Å of vacuum with full periodic boundary conditions representing an infinite Cu(111) surface. Each layer contained 64 copper atoms, and the size of the unit cell in the direction parallel to the surface was 14.46 × 14.46 $Å^2$. The Brillouin-zone integration was performed using a set of *k* points generated by the 2×2×1 Monkhorst-Pack mesh. We performed full geometry optimizations until the residual forces were less than 0.02 eV/Å. To compute reaction barriers, we used the NEB method with the 'climbing image' algorithm.[7] Activation barriers obtained with the NEB method refer to a temperature of 0 K. The reaction pathway by means of NEB calculations based on the constrained geometry optimizations. Therefore, all intermediate states were identified by a series of constrained geometry optimizations. Once a constraint is defined (e.g., the forces between atoms) a geometry optimization is performed to force the constraint to preserve a given value.

In addition, to provide more robustness to our calculations, we have considered the local-density-functional approximation (LDA)[3,8] for the exchange-correlation potential, which is also widely used for predicting the interaction of graphene with metal surface. [9] We find that the results and properties are similar to those obtained based on the PBE, just with slightly different values.

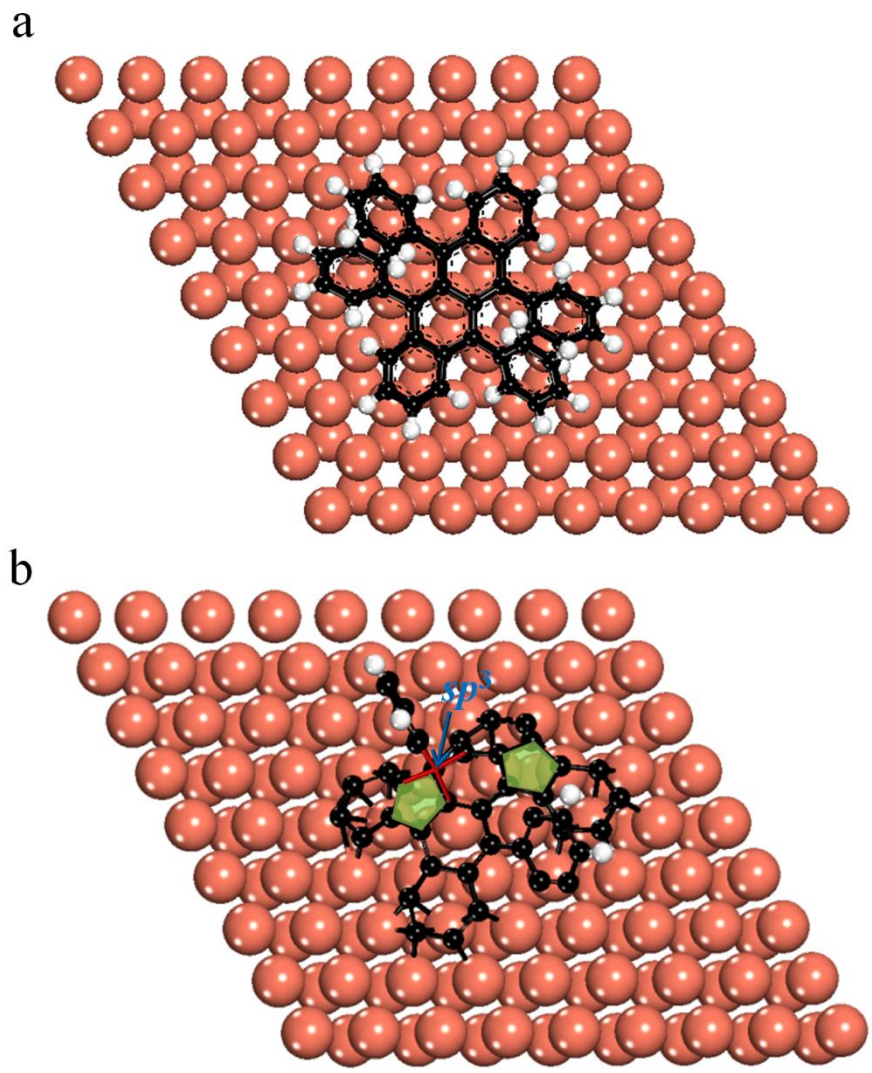

FIGURE S4. The configurations of intact and partial dehydrogenated rubrene molecules adsorbing on Cu (111) surface computed by DFT.

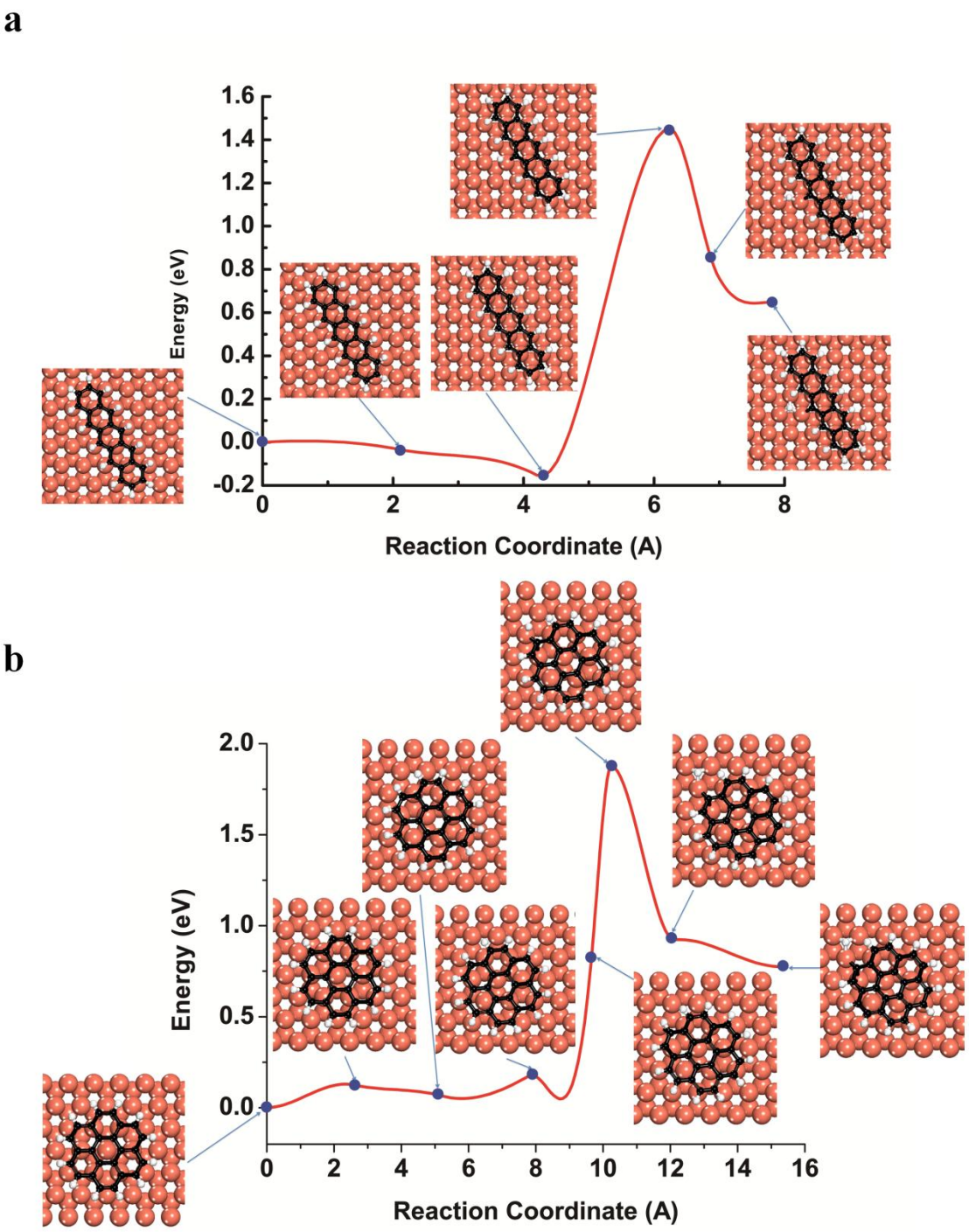

FIGURE S5. The minimum energy pathways including the transition state (TS) and intermediate geometry for the dehydrogenation of (a) pentacene and (b) coronene on Cu (111) surface. The minimum energy (for C–H scission) required to surmount the TS for pentacene is 1.46 eV and for coronene is 1.87eV on Cu (111) surface.

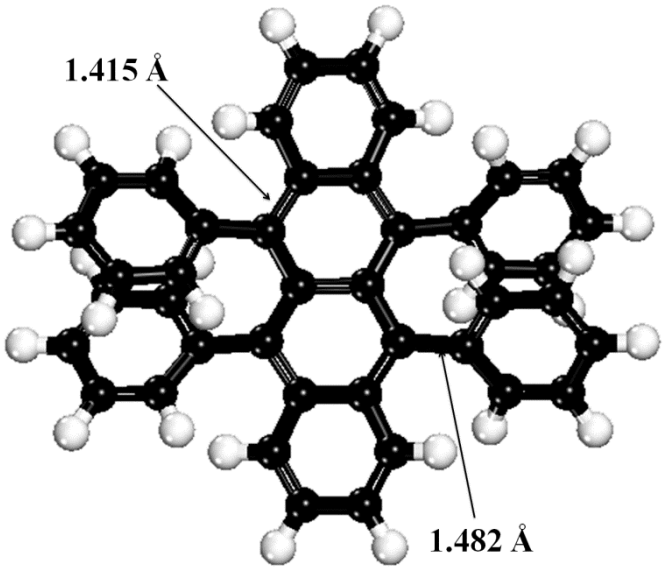

FIGURE S6. The structure of isolated rubrene molecule relaxed by DFT.

SI-3 Graphene growth on Ni films from rubrene.

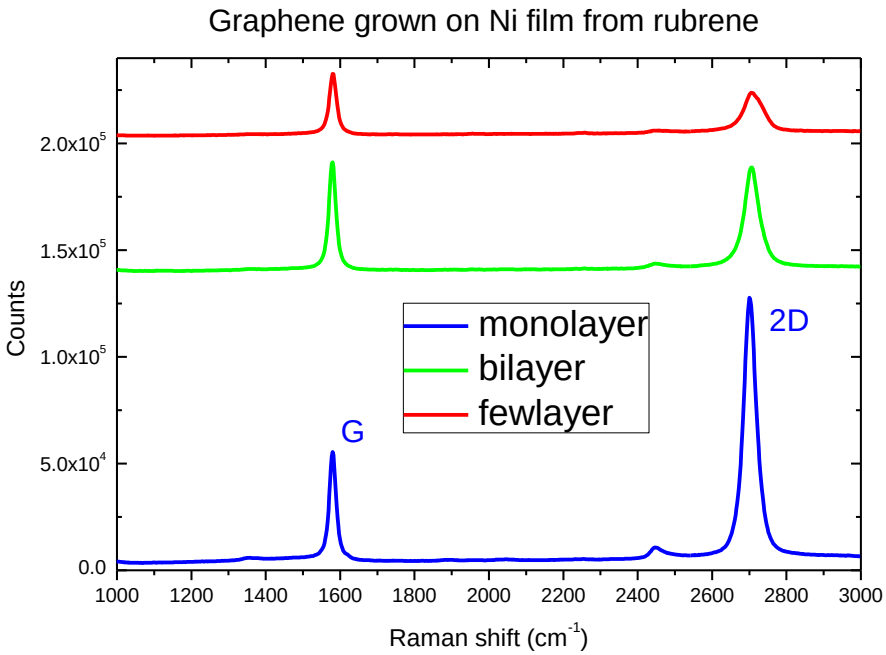

FIGURE S7 High-quality graphene sheets (one to few layers) with tiny *D* peaks can be synthesized on Ni films (~300nm, prepared by e-beam evaporation on SiO_2/Si wafer) from rubrene at 900˚C in a vacuum furnace similar to the one used by Li, *et.al*.[10]

Our finding is consistent with the previously reported growth mechanism in which the graphene growth on Ni substrate possesses a carbon segregation or precipitation process owing to the high carbon solubility in nickel (2.7%)[11] and the strong interaction (carbide) between C and Ni atoms.[12-14]

REFERENCES

(1) Park, H.; Brown, P. R.; Bulović, V.; Kong, J. *Nano Lett* **2011**.
(2) Hohenberg, P.; Kohn, W. *PHYSICAL REVIEW* **1964**, *136*, B864-B871.
(3) Kohn, W.; Sham, L. J. *PHYSICAL REVIEW* **1965**, *140*, A1133-A1138.
(4) Perdew, J. P.; Burke, K.; Ernzerhof, M. *Phys Rev Lett* **1996**, *77*, 3865-3868.
(5) Kresse, G.; Joubert, D. *Phys Rev B* **1999**, *59*, 1758-1775.
(6) Kresse, G.; Furthmüller, J. *Phys Rev B* **1996**, *54*, 11169-11186.
(7) Henkelman, G.; Uberuaga, B. P.; Jonsson, H. *J Chem Phys* **2000**, *113*, 9901-9904.
(8) Ceperley, D. M.; Alder, B. J. *Phys Rev Lett* **1980**, *45*, 566-569.
(9) Giovannetti, G.; Khomyakov, P. A.; Brocks, G.; Karpan, V. M.; van den Brink, J.; Kelly, P. J. *Phys Rev Lett* **2008**, *101*, 026803.
(10)Li, Z. C.; Wu, P.; Wang, C. X.; Fan, X. D.; Zhang, W. H.; Zhai, X. F.; Zeng, C. G.; Li, Z. Y.; Yang, J. L.; Hou, J. G. *Acs Nano* **2011**, *5*, 3385-3390.
(11) Liu, N.; Fu, L.; Dai, B.; Yan, K.; Liu, X.; Zhao, R.; Zhang, Y.; Liu, Z. *Nano Lett* **2011**, *11*, 297-303.
(12) Reina, A.; Jia, X.; Ho, J.; Nezich, D.; Son, H.; Bulovic, V.; Dresselhaus, M. S.; Kong, J. *Nano Lett* **2009**, *9*, 30-35.
(13) Li, X.; Cai, W.; Colombo, L.; Ruoff, R. S. *Nano Lett* **2009**, *9*, 4268-4272.
(14) Xu, M.; Fujita, D.; Sagisaka, K.; Watanabe, E.; Hanagata, N. *Acs Nano* **2011**, *5*, 1522-1528.